effects of melatonin are prevented by SCN lesions, and administration of melatonin alters metabolic activity and inhibits cell firing in the SCN of the rat and the Djungarian hamster[5,10,20,26]. *In vitro*, melatonin phase shifts the circadian rhythm of electrical activity in the rat SCN slices[27,28]. Thus these results suggest that melatonin induces phase shifts of circadian activity rhythms in the field mouse *M. booduga* by acting on melatonin receptors in the circadian oscillators.

1. Underwood, H., *Science*, 1977, **195**, 587–589.
2. Redman, J., Armstrong, S. and Ng, K. T., *Science*, 1983, **219**, 1089–1091.
3. Underwood, H., *J. Pineal Res.*, 1986, **3**, 187–196.
4. Heigl, S. and Gwinner, E., *Soc. Res. Biol. Rhythms*, 1992, **3**, 95.
5. Margraf, R. R. and Lynch, G. R., *Am. J. Physiol.*, 1993, **264**, R615–R621.
6. Redman, J. and Amstrong, S., *J. Pineal Res.*, 1988, **5**, 203–215.
7. Benloucif, S. and Dubocovich, M. L., *Soc. Neurosci. Abstr.*, 1994, **20**, 1438.
8. Dubocovich, M. L., Benloucif, S. and Masana, M. I., *Behav. Brain Res.*, 1996, **73**, 141–147.
9. Singaravel, M., Sharma, V. K., Subbaraj, R. and Nair N. G., *J. Biosci.*, 1996, **21**, 789–795.
10. Cassone, V. M., Chesworth, M. J. and Armstrong, S. M., *Physiol. Behav.*, 1986, **36**, 1111–1121.
11. Warren, W. S., Hodges, D. B. and Cassone, V. M., *J. Biol. Rhythms*, 1993, **8**, 233–245.
12. Cassone, V. M., *TINS*, 1990, **13**, 457–464.
13. Reppert, S. M., Weaver, D. R. and Ebisawa, T., *Neuron*, 1994, **13**, 1177–1185.
14. Armstrong, S. M., *Pineal Res. Rev.*, 1989, **7**, 157–202.
15. Lewy, A. J., Ahmed, S., Latham-Jackson, J. M. and Sack, R. L., *Chronobiol. Int.*, 1992, **9**, 380–392.
16. Benloucif, S. and Dubocovich, M. L., *J. Biol. Rhythms*, 1996, **11**, 113–125.
17. Golombek, D. A. and Cardinali, D. P., *Chronobiol. Int.*, 1993, **10**, 435–441.
18. Daan, S. and Pittendrigh, C. S., *J. Comp. Physiol.*, 1976, **106**, 253–266.
19. Tamarkin, L., Baird, C. L. and Almeida, O. F. X., *Science*, 1985, **227**, 714–725.
20. Cassone, V. M., Roberts, M. H. and Moore, R. Y., *Am. J. Physiol. (Reg. Integr. Comp. Physiol.)*, 1988, **255**, R332–R337.
21. Redman, J. R., *J. Biol. Rhythms*, 1997, **12**, 581–587.
22. Hastings, M. H., Mead, S. M., Vindlacheruvu, R. R., Ebling, F. J., Maywood, E. S. and Grosse, J., *Brain Res.*, 1992, **591**, 20–26.
23. Tenn, C. and Niles, L. P., *Mol. Cell Endocrinol.*, 1993, **98**, 43–48.
24. Masana, M. I., Benloucif, S., Dubocovich, M. L., *Soc. Neurosci. Abstr.*, 1995, **21**, 184.
25. Brooks, D. S. and Cassone, V. M., *Endocrinology*, 1992, **131**, 1297–1304.
26. Stehle, J. Vanecek, J. and Vollrath, L., *J. Neural. Trans. (Gen. Sect.)*, 1989, **78**, 173–177.
27. McArthur, A. J., Gillette, M. U. and Prosser, R. A., *Brain Res.*, 1991, **565**, 158–161.
28. Gillette, M. U. and McArthur, A. J., *Behav. Brain Res.*, 1996, **73**, 135–139.

ACKNOWLEDGEMENTS. We are grateful to Prof. M. K. Chandrashekaran and Dr G. Marimuthu for critically reading the manuscript. This work was supported by University Grants Commission, New Delhi to R.S. and CSIR-SRF to M.S.

Received 24 December 1997; revised accepted 24 April 1998

Seismic hazard analysis: An artificial neural network approach

Manoj Arora* and M. L. Sharma†,§

Departments of *Civil Engineering and †Earthquake Engineering, University of Roorkee, Roorkee 247 667, India

An artificial neural network (ANN) approach is applied for the estimation of seismic hazard in a region. The seismicity rhythm is recognized by means of an ANN approach. The seismicity cycle may be divided into four stages, viz. energy accumulation, increasing release in energy, intense release and the remnant release of seismic energy. The seismicity data from the earthquake catalogue (1790–1990) for the Arakan Yoma and Naga Thrust belt in NE India have been used. Future seismicity for the region is predicted up to the year 2040. The results show that the intense energy release cycle will start somewhere in the year 2030 and will continue up to 2040. The successful operation of ANN and its application to predict seismicity cycle in the selected region shows that the approach may be applied to other areas also for the seismic hazard evaluation.

THE seismic hazard in a region may be defined as the probability of occurrence of earthquake given in units of a certain level of vibrations expected in a particular region within a certain period of time. The final result of the seismic hazard analysis is the determination of the probability of occurrence of natural phenomenon (intensity, magnitude, accelerations, etc.). For such analysis, statistical characteristics of seismic hazard are generally applied. The observations from the past (seismicity) records are used to model the future activity. A variety of statistical procedures may be applied at various stages of the formulation and evaluation of proposed models which, besides the stationary Poisson process, include: Baysian methods facilitating the incorporation of diverse elements of uncertainty and combining estimates by different models; semi-Markov process applied to linear zones; stochastic models and/or clustering for cyclic fluctuation and other trends; models based on precursory phenomena, which consider the probability distribution for magnitude, location and time of occurrence of predicted earthquakes[1]. These methods may be appropriate to reveal some statistical characteristics of seismic hazard, but may not provide a direct quantitative evaluation. In practice, an appropriate assessment usually needs further comprehensive judgements based on experience.

New methods are, therefore, to be introduced to overcome the limitations of conventional methods. Artificial neural network (ANN) approach has recently been touted as having enormous potential for a variety of problems in various fields such as image and signal processing,

§For correspondence. (e-mail: civil@rurkiu.ernet.in)

civil, electrical and mechanical engineering. This is primarily due to the fact that this approach does not depend upon any assumptions about the distribution of data, has the ability to handle data obtained at different levels of precision, and has rapid data processing capability. In the present context, this approach has been applied to evaluate the seismic hazard. To testify the significance of this approach, the Indo-Burma seismic region has been selected to predict the seismicity cycle for the region.

An artificial neural network may be considered to comprise of a relatively large number of simple processing units (nodes) that work in parallel to evaluate the seismicity fluctuation in the time series from historical data[2]. These processing units are generally organized into layers, each unit in a layer being connected to every other unit in the following layer. This is known as feedforward multi-layer[3].

The architecture of a typical multi-layer ANN is shown in Figure 1. It consists of an input layer, a hidden layer and an output layer. The input layer is passive and merely receives the data (e.g. historical seismicity cycles data)[4]. Consequently, the units in the input layer equal the number of variables to be used to predict the values for the future seismicity cycle (e.g., the characteristics values for various stages of seismicity cycle for a time series). Unlike input layer, both hidden and output layers actively process the data. The output layer produces the neural network's results. In the present context, the result denotes the predicted values of siesmicity cycle over a certain period of time. Thus, the number of units in the output layer corresponds to the predicted characteristic values for the number of stages of seismicity cycles of interest. Hence, the number of units in the input and the output layers are typically fixed by the application designed[5]. Introducing hidden layer between input and output layer increases the network's ability to model complex functions[4]. Selection of appropriate number of hidden layers and their units is critical for the operation of the neural network. With too few hidden units, the network may not be powerful enough for its processing while with a large number of hidden units, computation becomes expensive. The optimal number of hidden units is often determined experimentally using a trial and error method although some basic geometrical arguments may be used to obtain an approximate indication.

The units in the neural network are an abstraction of the biological concept of a neuron and weighted paths

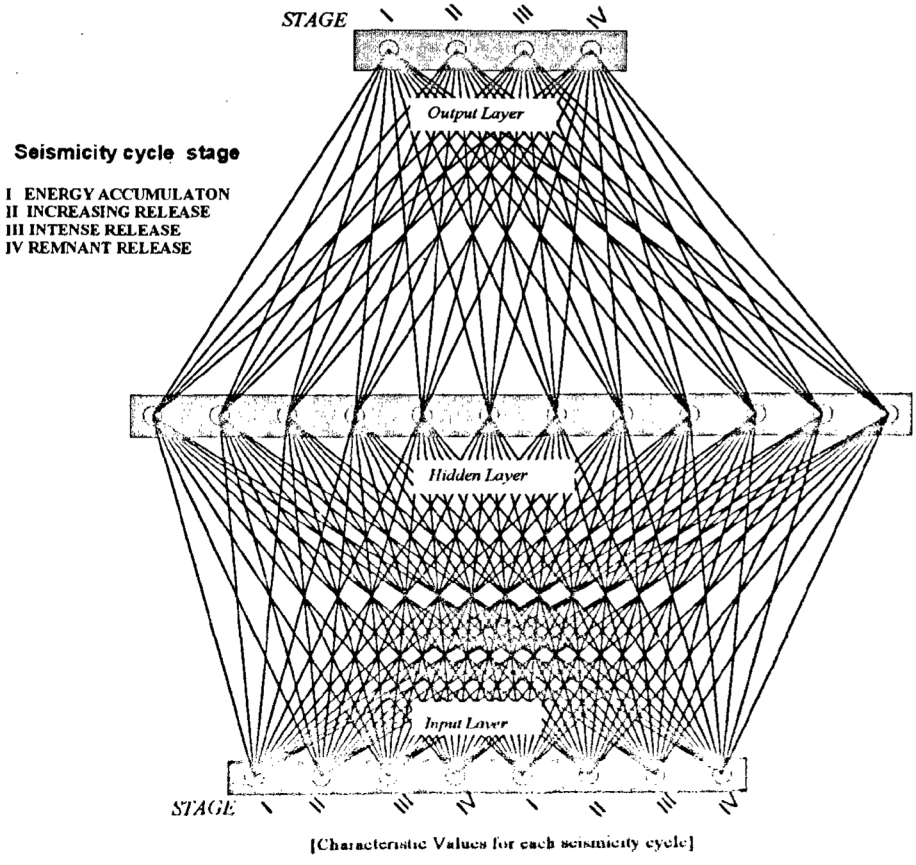

Figure 1. Overview of prediction of seismicity cycle with an artificial neural network.

connecting these units[6]. Signals impinging on a unit's input are multiplied by the path's weight and are summed to derive the net input to that unit. The net input (*NET*) is then transformed by an activation function (f) to produce an output for the unit. The most common form of the activation function is a Sigmoid function, defined as,

$$f(NET) = 1/1 - e^{-NET} \quad (1)$$

and accordingly,

$$\text{Output} = f(NET), \quad (2)$$

where *NET* is the sum of the weighted inputs to the processing unit and may be expressed as

$$NET = \sum_{i=1}^{n} x_i w_i \quad (3)$$

where x_i is the magnitude of the ith input and w_i is the weight of the interconnected path.

The determination of the appropriate weights is referred to as learning or training. Learning algorithms may be categorized as supervised and unsupervised[7]. Generally a backpropagation algorithm is applied which is a supervised algorithm and has been widely used in neural network applications. The algorithm iteratively minimizes an error function over the network outputs and a set of target outputs, taken from the training data set. The process continues until the error value converges to a minima. Conventionally, the error function is given as,

$$E = 0.5 \sum_{i=1}^{c} (T_i - O_i)^2, \quad (4)$$

where T_i is the target output vector and O_i is the network output.

Thus, the magnitudes of the weights are determined by an iterative training procedure in which the network repeatedly tries to learn the correct output for each training sample. The procedure involves modifying the weights between units until the network is able to characterize the training data.

Once the training is complete, the network has memorized the knowledge contained in the data set in the form of adjusted weights. In order to evaluate the performance of the neural network approach, this knowledge in the form of weights is then used to process a data sample whose target values are also known similar to the training data. This data sample is known as testing data. If the performance of the network on testing data sets is found to be satisfactory, the network is supposed to have a generalization capability over any other set of similar data. Once tested successfully, the trained network may be used to process the unknown data in order to predict the characteristic values for those data sets.

The north-eastern part of the Indian plate and northern part of the Burma plate extend between 20°N to 30°N and 88°E to 100°E. The geological set up and seismotectonics of this region is extremely complex[8–10]. The region consists of four tectonic units, viz. eastern syntaxis (zone I), the Arakan Yoma and Naga thrust fold belt (zone II), the Shillong plateau (zone III), and the MCT and MBT faults of the Himalayan Frontal arc (zone IV). The seismic activity of this region is a consequence of collision tectonics in the Himalayas and the subduction tectonics below the Burmese plate and is associated with a few major geological units. The fluctuation of seismicity in most part of the Eastern Himalayas, especially in the eastern side, is well known[11], but its regularity may not be described by any mathematical model.

The area selected for the present study lies between 20°N to 27.5°N and 93°E to 98°E and includes zone II defined above (Figure 2). The nature of faulting is different in different seismotectonic elements. However, the overall seismicity of the region is assumed to be dependent on the resistance offered by each element (zone) and the stress generated as a consequence.

The seismicity of the area considered is plotted in Figure 3, which shows a cyclic behaviour. It is generally assumed that the seismicity cycle in an area consists of four stages, viz. (i) energy accumulation stage, (ii) increasing release of energy stage, (iii) intense release of energy stage, and (iv) remnant release of energy stage. From Figure 3, it can also be seen that the first seismicity cycle ranges from 1790 to 1890 and the other from 1890 to 1990. The year 1790 has been assumed as the start of the first cycle based on the behaviour of preceding cycle as the historical data may not be reported in the past. The four stages have been marked in Figure 3.

For seismic hazard analysis using ANN, a time interval of 50 years was chosen as one input segment. A characteristic value was assigned to each of the four stages (as defined above) in this segment. This characteristic value corresponds to the time taken by a particular stage normalized by the total time interval of the segment, i.e. 50 years. Thus, one complete cycle of the seismicity contained two segments having four characteristic values for each. If a particular stage did not appear in the segment, it has been assigned a characteristic value 0.

These characteristic values for the region selected are given in Table 1. Thus the input layer of ANN consists of 8 units representing the characteristic values for two segments. The number of units in the hidden layer was determined by trial and error. The 4 units of the output layer comprised of characteristic values of one segment

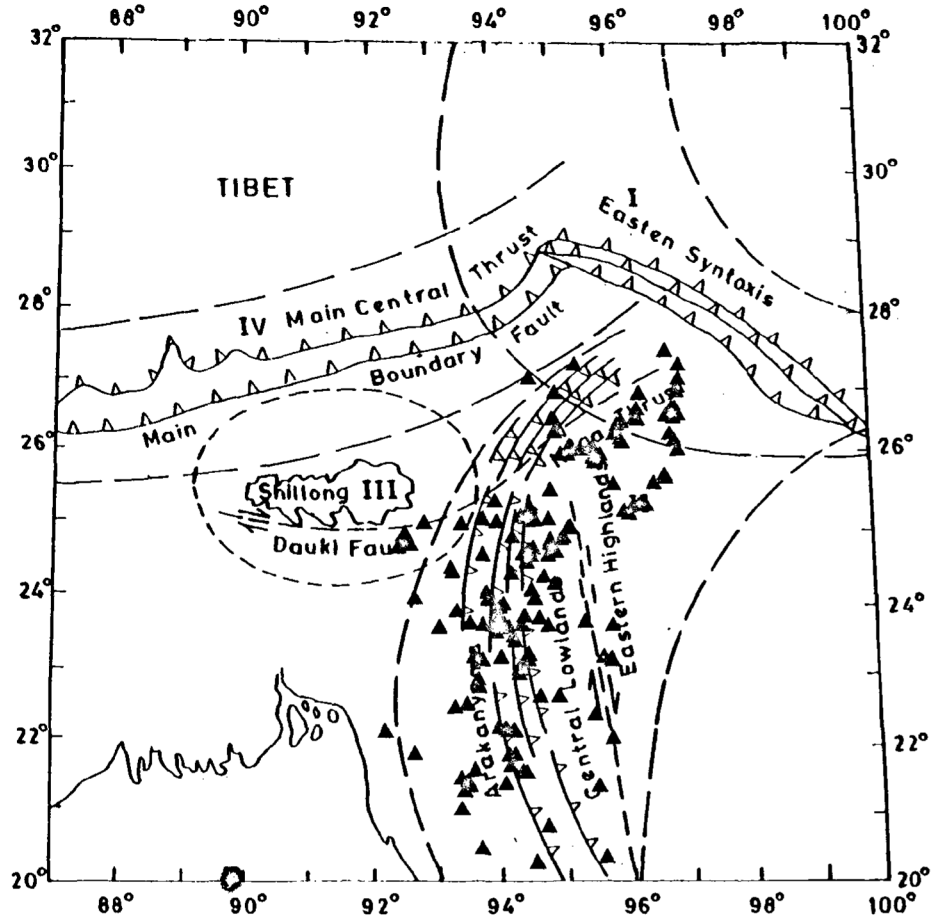

Figure 2. Earthquake occurrence in the Arakan Yoma–Naga Thrust Fold Belt. (For magnitudes refer Figure 3).

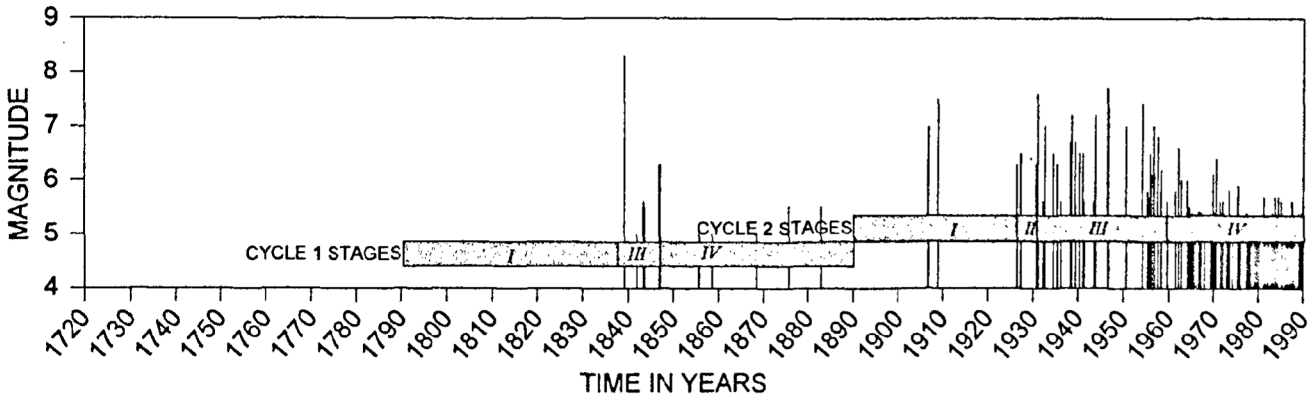

Figure 3. Magnitude–time period plot and seismicity cycles stages of the Arakan Yoma–Naga Thrust Fold Belt.

for the next 50 years. For instance, from 1790 to 1890 (100 years), the characteristic values for the 8 input units are 0.94, 0.00, 0.06, 0.00, 0.00, 0.00, 0.16, 0.84 respectively, while the values for the 4 output units are 0.74, 0.06, 0.20, 0.00, which correspond to the time interval between 1890 and 1940 (50 years). In order to generate training and testing, samples for a shift of 5 years were taken for a 100-years moving window. The characteristic values for the period 1790 to 1990 thus generated with a shift of 5 years, are shown in Table 2. A total of 21 samples were generated. Of these, the characteristic values for both input and output units were available for 11 samples (i.e. 1790 to 1940) only. First 6 samples were used for training the ANN and

the remaining 5 samples were used for testing the ANN. The network was trained in 50,000 iterations with a learning and momentum rate of 0.1 and 0.1 respectively with an acceptable error of 0.000642 (eq. (4)).

The weights obtained after training the network were used to determine the characteristic values at the output units for testing samples (Table 3). The testing samples have been taken for the year 1820 to 1940. The observed and computed values are also given in Table 3. It can be seen that there is no significant difference between the observed and the computed values. This shows that the network has obtained the generalization capability also and thus it can be used to process any other data in this region.

The data generated from the historical seismicity in the form of characteristic values for the four stages of the seismicity cycles are used to compute future trends in the seismicity cycles. The data from 1845 to 1990 have been used for computation of seismicity cycles up to the year 2040. The computed characteristic values from ANN along with the input and output time periods are given in Table 4. These characteristic values for the four stages were converted back to the years by multiplying each value by 50 years.

It has been found that the characteristic value for stage I (the energy accumulation) is increasing with time. This indicates that the energy accumulation stage of the seismicity cycle will take place up to the year 2025 so that there will be less number of earthquakes of higher magnitude during this period. The stage II (increasing seismic activity stage) is having almost uniform characteristic values indicating that this stage, will be common to all the moving windows and will fall in the middle of the time period, i.e. somewhere around 2025 to 2030 for 2–4 years. The next stage, which is the intense release stage, will start from 2030 and will

Table 1. Characteristic values for the sliding windows of the seismicity cycles for four stages of each cycle

Time period	Characteristic values (Stages)							
	I	II	III	IV	I	II	III	IV
1790–1890	0.94	0.00	0.06	0.00	0.00	0.00	0.16	0.84
1795–1895	0.84	0.00	0.16	0.00	0.10	0.00	0.06	0.84
1800–1900	0.74	0.00	0.22	0.04	0.20	0.00	0.00	0.80
1805–1905	0.64	0.00	0.22	0.14	0.30	0.00	0.00	0.70
1810–1910	0.54	0.00	0.22	0.24	0.40	0.00	0.00	0.60
1815–1915	0.44	0.00	0.22	0.34	0.50	0.00	0.00	0.50
1820–1920	0.34	0.00	0.22	0.44	0.60	0.00	0.00	0.40
1825–1925	0.24	0.00	0.22	0.54	0.70	0.00	0.00	0.30
1830–1930	0.14	0.00	0.22	0.64	0.74	0.06	0.00	0.20
1835–1935	0.04	0.00	0.20	0.74	0.74	0.06	0.10	0.10
1840–1940	0.00	0.00	0.16	0.84	0.74	0.06	0.20	0.00
1845–1945	0.10	0.00	0.06	0.84	0.64	0.06	0.30	0.00
1850–1950	0.20	0.00	0.00	0.80	0.54	0.06	0.40	0.00
1855–1955	0.30	0.00	0.00	0.70	0.44	0.06	0.50	0.00
1860–1960	0.40	0.00	0.00	0.60	0.34	0.06	0.60	0.00
1865–1965	0.50	0.00	0.00	0.50	0.24	0.06	0.60	0.10
1870–1970	0.60	0.00	0.00	0.40	0.14	0.06	0.60	0.20
1875–1975	0.70	0.00	0.00	0.30	0.04	0.06	0.60	0.30
1880–1980	0.74	0.06	0.00	0.20	0.00	0.00	0.60	0.40
1885–1985	0.74	0.06	0.10	0.10	0.00	0.00	0.50	0.50
1890–1990	0.74	0.06	0.20	0.00	0.00	0.00	0.40	0.60

Table 2. Training of artificial neural network

Time period			Characteristic values (Stages)			
Input	Output		I	II	III	IV
1790–1890	1890–1940	O	0.74	0.06	0.20	0.00
		C	0.73	0.06	0.21	0.00
1795–1895	1895–1945	O	0.64	0.06	0.30	0.00
		C	0.65	0.06	0.29	0.00
1800–1900	1900–1950	O	0.54	0.06	0.40	0.00
		C	0.54	0.06	0.40	0.00
1805–1905	1905–1955	O	0.44	0.06	0.50	0.00
		C	0.44	0.06	0.50	0.01
1810–1910	1910–1960	O	0.34	0.06	0.60	0.00
		C	0.33	0.06	0.58	0.03
1815–1915	1915–1965	O	0.24	0.06	0.60	0.10
		C	0.24	0.06	0.61	0.08

O, Observed; C, Computed.

Table 3. Testing of the data

Time period			Characteristic values (Stages)			
Input	Output		I	II	III	IV
1820–1920	1920–1970	O	0.14	0.06	0.60	0.20
		C	0.17	0.06	0.60	0.17
1825–1925	1925–1975	O	0.04	0.06	0.60	0.30
		C	0.12	0.06	0.56	0.27
1830–1930	1930–1980	O	0.00	0.00	0.60	0.40
		C	0.10	0.06	0.52	0.32
1835–1935	1935–1985	O	0.00	0.00	0.50	0.50
		C	0.10	0.06	0.50	0.33
1840–1940	1940–1990	O	0.00	0.00	0.40	0.60
		C	0.12	0.06	0.49	0.34

O, Observed; C, Computed.

Table 4. Results of the AI analysis for eleven stages of the characteristic values of seismicity cycles

Time period			Characteristic values (Stages)			
Input	Output		I	II	III	IV
1845–1945	1945–1995	C	0.20	0.05	0.49	0.26
1850–1950	1950–2000	C	0.32	0.05	0.50	0.13
1855–1955	1955–2005	C	0.42	0.05	0.47	0.06
1860–1960	1960–2010	C	0.52	0.05	0.42	0.01
1865–1965	1965–2015	C	0.57	0.05	0.38	0.00
1870–1970	1970–2020	C	0.63	0.07	0.30	0.00
1875–1975	1975–2025	C	0.70	0.07	0.23	0.00
1880–1980	1980–2030	C	0.72	0.04	0.24	0.00
1885–1985	1985–2035	C	0.71	0.03	0.26	0.00
1890–1990	1990–2040	C	0.70	0.02	0.28	0.00

C, Computed.

continue up to 2040, showing that this period will experience high magnitude occurrence. This aspect has also been verified by the return period of the higher magnitude earthquakes and their probability of occurrence during this period[12]. The stage IV, which is the remnant energy release stage will start after 2040 as clear from the computed characteristic values for this stage which are 0 for this time period in the windows starting from the 1970–2020 to 1990–2040.

1. Rhodes, D. A., 23rd General Assembly of IASPEI, Tokyo, August, 19–30, Abstract, 1985, vol. 1, p. 14.
2. Xianxin, T., Wei, D. and Guangfen, Z., Proceedings of Ist International Conference on Seismology Earthquake Enggineering, May 27–29, 1991, pp. 257–266.
3. Schalkoff, R. J., *Pattern Recognition: Statistical, Structural and Neural Approaches*, Wiley, New York, 1992.
4. Hammerstrom, D., *IEEE Spectrum*, 1993, **30**, 46–53.
5. Arora, M., Ph D thesis, University of Wales, UK, 1996.
6. Lee, J., Weger, R. C., Sengupta, S. K. and Welch, R. M., *IEEE Trans. Geosci. Remote Sensing*, 1990, **28**, 846–855.
7. Foody, G. M., *Int. J. Geograph. Inf. Systems*, 1995, **9**, 527–542.
8. Nandy, D. R., *J. Earth. Sci.*, 1980, **7**, 103–107.
9. Desikochar, S. K., *J. Geol. Soc. India*, 1974, **15**, 137–149.
10. Evans, P., *J. Geol. Soc. India*, 1974, **5**, 80–96.
11. Shanker, D. and Singh, V. P., *Sci. Cult.*, 1996, **62**, 215–217.
12. Shanker, D. and Sharma, M. L., Proceedings of Workshop on Earthquake Disaster Preparedness, Oct. 13–14, Roorkee, 1997, pp. 49–58.

Received 6 January 1998; accepted 6 April 1998

MEETINGS/SYMPOSIA/SEMINARS

Tenth National Conference of Society for Biomaterials and Artificial Organs – India

Date: 9–10 November 1998
Place: Thiruvananthapuram

The technical programme covers invited talks, oral presentation and poster presentation in the following areas: Biomedical polymers, ceramics and metals, artificial organs, tissue engineering, soft tissue implants, hard tissue implants, drug delivery devices, biomedical devices safety, biomedical ethics, clinical issues on medical devices, biomedical devices standards and good manufacturing practices and challenges in biomedical device industry.

Contact: Dr M. Jayabalan
Organizing Secretary, NCSBAO-98
Polymer Division, BMT Wing
Sree Chitra Tirunal Institute for
Medical Sciences and Technololgy
Thiruvananthapuram 695 012
Phone: (0471) 340801 (O), (04651) 60624 (R)
Fax: (0471) 341814
E-mail: bmtwing@md2.vsnl.net.in

4th International Symposium on Genetics, Health and Diseases

Date: 1–4 December 1998
Place: Amritsar, India

Contact: Prof. Jai Rup Singh
Co-ordinator
International Symposium on Genetics,
Health and Diseases
Department of Human Genetics
Guru Nanak Dev University
Amritsar 143 005, India
Phone: (0183) 258802 to 09 extn 3277
Fax: (0183) 258863/258820

XXIX National Seminar on Crystallography

Date: 23–25 December 1998
Place: Chennai

Topics include: Methods, Biocrystallography, Materials Science, Real and ideal crystals, Inorganic and mineralogical crystallography, Apparatus and techniques, Structure methods and other than diffraction, Structures of organic, organometallic compounds, Education and data retrieval.

Contact: Prof. Vasantha Pattabhi
Department of Biophysics
University of Madras, Guindy Campus
Chennai 600 025
Phone: (044) 2300122, 2351367 extn 211
Fax: (044) 2352494
E-mail: crystal@giasmd01.vsnl.net.in